Optimized Schwarz Preconditioning for SEM Based Magnetohydrodynamics

Amik St-Cyr[1], Duane Rosenberg[1], and Sang Dong Kim[2]

[1] Institute for Mathematics Applied to Geosciences, National Center for Atmospheric Research, Boulder, CO, USA: {amik,duaner}@ucar.edu
[2] Department of Mathematics, Kyungpook National University, Daegu 702-701, South Korea: skim@knu.ac.kr.

Summary. A recent theoretical result on optimized Schwarz algorithms, demonstrated at the algebraic level, enables the modification of an existing Schwarz procedure to its optimized counterpart. In this work, it is shown how to modify a bilinear finite-element method based Schwarz preconditioning strategy originally presented in [6] to its optimized version. The latter is employed to precondition the pseudo-Laplacian operator arising from the spectral element discretization of the magnetohydrodynamic equations in Elsässer form.

1 Introduction

This work concerns the preconditioning of a pseudo-Laplacian operator[3] associated with the saddle point problem arising at each time-step in a spectral element based adaptive MHD solver. The approach proposed is a modification of the method developed in [6] where an overlapping Schwarz preconditioner for the pseudo-Laplacian was constructed using a low order discretization of the weak Laplacian. The finite-element blocks, representing the additive Schwarz, are replaced by so called optimized Schwarz blocks [12]. Two types of overlapping subdomains, employed to construct the finite-element block preconditioning are investigated. The first one is cross shaped and shows good behavior for additive Schwarz (AS) and restricted additive Schwarz (RAS). Improved convergence rates of the optimized RAS (ORAS) version are completely dominated by the corner effects [2]. Opting for a second grid that includes the corners seems to correct this issue. For the zeroth order optimized transmission condition (OO0) an exact tensor product form is available while for the second order version (OO2) version a slight error is introduced in order to preserve the properties of the operators and enable the use of fast diagonalization techniques (FDM) [3].

[3] A.k.a: consistent Laplacian or approximate pressure Schur complement.

2 Governing Equations and Discretization

For an incompressible fluid with constant mass density ρ_0, in two spatial dimensions, the magnetohydrodynamic (MHD) equations are:

$$\partial_t \mathbf{u} + \mathbf{u}\cdot\nabla\mathbf{u} = -\nabla p + \nabla\times\mathbf{b}\times\mathbf{b} + \nu\nabla^2\mathbf{u}, \tag{1}$$

$$\partial_t \mathbf{b} = \nabla\times(\mathbf{u}\times\mathbf{b}) + \xi\nabla^2\mathbf{b} \tag{2}$$

$$\nabla\cdot\mathbf{u} = 0, \qquad \nabla\cdot\mathbf{b} = 0 \tag{3}$$

$$\mathbf{u}(\mathbf{x},t=0) = \mathbf{u}_i, \;\; \mathbf{b}(\mathbf{x},t=0) = \mathbf{b}_i; \quad \mathbf{u}(\mathbf{x},t)|_{\partial\mathbb{D}} = \mathbf{u}^b, \;\; \mathbf{b}(\mathbf{x},t)|_{\partial\mathbb{D}} = \mathbf{b}^b \tag{4}$$

where $\mathbf{u}$ and $\mathbf{b}$ are the velocity and magnetic field (in Alfvén velocity units, $\mathbf{b} = \mathbf{B}/\sqrt{\mu_0\rho_0}$ with $\mathbf{B}$ the induction and μ_0 the permeability); p is the pressure divided by the (constant) mass density, ρ_0, and ν and ξ are the kinematic viscosity and the magnetic resistivity. In the closed domain $\mathbb{D}$, these equations are solved in Elsässer form [5]:

$$\partial_t \mathbf{Z}^{\pm} + \mathbf{Z}^{\mp}\cdot\nabla\mathbf{Z}^{\pm} + \nabla p - \nu^{\pm}\nabla^2\mathbf{Z}^{\pm} - \nu^{\mp}\nabla^2\mathbf{Z}^{\mp} = 0 \tag{5}$$

$$\nabla\cdot\mathbf{Z}^{\pm} = 0\,, \tag{6}$$

with $\mathbf{Z}^{\pm} = \mathbf{u}\pm\mathbf{b}$ and $\nu^{\pm} = \frac{1}{2}(\nu\pm\eta)$. The initial and boundary conditions for $\mathbf{Z}^{\pm}$ are trivially specified in terms of (4); we do not provide them here. The velocity $\mathbf{u}$ and magnetic field $\mathbf{b}$ can be recovered by expressing them in terms of $\mathbf{Z}^{\pm}$. For spatial discretization of (5)-(6), a $\mathbb{P}_N - \mathbb{P}_{N-2}$ spectral element formulation is chosen to prevent the excitation of spurious pressure modes. In the latter formalism, the domain $\mathbb{D}$ is composed of a union of non-overlapping quadrangles, $\mathbf{E}_k$: $\mathbb{D} \supseteq \bigcup_{k=1}^{K}\mathbf{E}_k =: \mathcal{T}_h$ where $\mathbf{P}_N = \{v_h \in L^2(\mathbb{D}) \mid v_h|_{\mathbf{E}_k}\circ T_{\mathbf{E}_k} \in (\mathbb{P}_N\otimes\mathbb{P}_N)(\mathbf{E}_k)\;\forall\;\mathbf{E}_k\in\mathcal{T}_h\}$ and $T_{\mathbf{E}_k}$ is the image of the reference element $[-1,1]\times[-1,1]$. Finally $\mathbf{P}_N$ and the space $\mathbf{U}_\gamma := \{\mathbf{w}\in(H^1(\mathbb{D}))^2 |\; \mathbf{w} = \gamma \text{ on } \partial\mathbb{D}\}$, with the usual definition for $H^1(\mathbb{D})$, are employed to define finite dimensional representations of $\mathbf{Z}^{\pm}$ (and $\mathbf{u}$, $\mathbf{b}$), p and test functions, $\zeta^{\pm}$ and q:

$$\mathbf{Z}_h^{\pm}\in\mathbf{U}^N = \mathbf{U}_{\mathbf{Z}^b}\bigcap(\mathbf{P}_N\cap C^0(\mathbb{D}))^2, \quad \zeta_h^{\pm}\in\mathbf{U}_0^N = \mathbf{U}_{\mathbf{0}}\bigcap(\mathbf{P}_N\cap C^0(\mathbb{D}))^2,$$
$$p_h,\, q_h \in \mathbf{Y}_0^{N-2} = L_0^2(\mathbb{D})\bigcap\mathbf{P}_{N-2}, \tag{7}$$

see for instance [9][4]. The basis for the velocity expansion in $\mathbf{P}_N\cap C^0(\mathbb{D})$ is the set of Lagrange interpolating polynomials on the Gauss-Lobatto-Legendre (GL) quadrature nodes, and the basis for the pressure is the set of Lagrange interpolants on the Gauss-Legendre (G) quadrature nodes $\{\eta_l\}_{l=0}^{N-2}$. The functions in $\mathbf{U}^N$ and $\mathbf{Y}_0^{N-2}$ are represented as expansions in terms of tensor products of basis functions within each subdomain $\mathbf{E}_k$. Substituting these (Galerkin) truncations into the variational form of (5)-(6), and using appropriate quadrature rules, we arrive at a set of semi-discrete equations written in terms of spectral element operators:

[4] $L_0^2(\mathbb{D}) := \{p\in L^2(\mathbb{D}) \mid \int_{\mathbb{D}} p = 0\}$ which fixes the null space for the pressure.

$$\mathsf{M}\frac{d\widehat{\boldsymbol{Z}}_j^{\pm}}{dt} = -\mathsf{M}\mathsf{C}^{\mp}\widehat{\boldsymbol{Z}}_j^{\pm} + \mathsf{D}_j^{\mathrm{T}}\widehat{\boldsymbol{p}}^{\pm} - \nu_{\pm}\mathsf{L}\widehat{\boldsymbol{Z}}_j^{\pm} - \nu_{\mp}\mathsf{L}\widehat{\boldsymbol{Z}}_j^{\mp} \tag{8}$$

$$\mathsf{D}^j\widehat{\boldsymbol{Z}}_j^{\pm} = 0, \tag{9}$$

for the j^{th} ($\in [1,\cdots,d]$) component. The variables $\widehat{\boldsymbol{Z}}^{\pm}$ represent the time-dependent coefficients of the polynomial expansions of $\mathbf{Z}_h^{\pm}$ collocated at the GL node points, and $\widehat{\boldsymbol{p}}^{\pm}$ are values of the pressure coefficients at the G node points. Hence, in this discretization vector quantities reside on a different mesh than the pressures leading to a staggered formulation. Note that because the constraints (6), are enforced separately on $\mathbf{Z}^{\pm}$, Eq. (8) contains a different pressure for *each* Elsässer vector. This essentially adds a pressure force, $-\frac{1}{2}\nabla(p^+ + p^-)$, to the momentum equation, and an electromotive force, $-\frac{1}{2}\nabla(p^+ - p^-)$, to the induction equation. In effect, we add a Lagrange variable to the induction equation, in the same way that it already exists for the velocity, such that $\nabla\cdot\mathbf{B} = 0$ in its discrete form–a form of *divergence cleaning* that renders the gradient (curl) and divergence operators consistent numerically. Note that if $\widehat{\boldsymbol{p}}^+ = \widehat{\boldsymbol{p}}^-$, the discrete approximation faithfully reproduces the continuous equations; in practice we find good agreement between these fields. The operators M, L, and C, are the well-known mass matrix, weak Laplacian and advection operators, respectively (*c.f.* [4]), and D_j represent the Stokes derivative operators, in which the GL basis function and its derivative operator are interpolated to the G node points, and multiplied by the G quadrature weights. All two dimensional operators are computed as tensor products of their component 1D operators. We note the effect of D_j, on (vector) quantities in $\mathbf{U}^N$: they take a derivative that itself resides on the G nodes; hence, the discrete divergence (9) is collocated on the same grid as the discrete pressure. The effect of the transposed Stokes operator $\mathsf{D}_j^{\mathrm{T}}$, on the other hand, is to compute a derivative of a $\mathbf{Y}^{N-2}$ quantity, which will be collocated with the $\mathbf{Z}^{\pm}$, $\mathbf{u}$, and $\mathbf{b}$. For time marching, we employ a simple second-order Runge-Kutta scheme (RK2) [1, p. 109]. The complete time discretization at each stage is (from 8):

$$\widehat{\boldsymbol{Z}}_j^{\pm,k} = \widehat{\boldsymbol{Z}}_j^{\pm,n} - \frac{k}{2}\Delta t\mathsf{M}^{-1}\left(\mathsf{M}\mathsf{C}^{\mp}\widehat{\boldsymbol{Z}}_j^{\pm,k-1} - \mathsf{D}_j^{\mathrm{T}}\widehat{\boldsymbol{p}}^{\pm,k-1} + \nu_{\pm}\mathsf{L}\widehat{\boldsymbol{Z}}_j^{\pm,k-1} + \nu_{\mp}\mathsf{L}\widehat{\boldsymbol{Z}}_j^{\mp,k-1}\right) \tag{10}$$

where $k = 1$ for the first stage and $k = 2$ for the last one[5]. We require that each stage satisfy (9) in its discrete form, so multiplying (10) by D^j, summing over j, and setting the term $\mathsf{D}^j\widehat{\boldsymbol{Z}}_j^{\pm} = 0$, we arrive at the following pseudo-Poisson equation for the pressures, $\widehat{\boldsymbol{p}}^{\pm,k-1}$:

$$E\widehat{\boldsymbol{p}}^{\pm,k-1} := \mathsf{D}^j\mathsf{M}^{-1}\mathsf{D}_j^{\mathrm{T}}\widehat{\boldsymbol{p}}^{\pm,k-1} = \mathsf{D}^j\widehat{\boldsymbol{g}}_j^{\pm,k-1}\,, \tag{11}$$

where, for completeness, the quantity

[5] $\widehat{\boldsymbol{Z}}_j^{\pm,k=0} := \widehat{\boldsymbol{Z}}_j^{\pm,n}$ and $\widehat{\boldsymbol{Z}}_j^{\pm,n+1} := \widehat{\boldsymbol{Z}}_j^{\pm,k=2}$

$$\widehat{\boldsymbol{g}}_j^{\pm,k-1} = \frac{1}{k}\Delta t\, \mathsf{M}^{-1}\big(\mathsf{M}\mathsf{C}^{\mp}\widehat{\boldsymbol{Z}}_j^{\pm,k-1} + \nu_{\pm}\mathsf{L}\widehat{\boldsymbol{Z}}_j^{\pm,k-1} + \nu_{\mp}\mathsf{L}\widehat{\boldsymbol{Z}}_j^{\mp,k-1}\big) - \widehat{\boldsymbol{Z}}_j^{\pm,n}$$

is the remaining inhomogeneous contribution (see [11]). In general, we are interested in high Reynolds number—where ν and η tend to zero—solutions of (5)-(6) (or (8)-(9)), for which the nonlinear terms $\mathbf{Z}^{\mp}\cdot\nabla\mathbf{Z}^{\pm}$ (or $\mathbf{C}^{\mp}\widehat{\boldsymbol{Z}}_j^{\pm}$) dominate the viscous terms. We note that explicit time-stepping presents no problem if the Courant restriction is not violated. Equation (11) is solved using a preconditioned iterative Krylov method, and our focus in the remainder of this paper concerns the preconditioning of this system.

3 From Classical to Optimized Schwarz

The principle behind optimized Schwarz methods consists of replacing the Dirichlet *transmission* condition present in the classical Schwarz approach by a more general Robin boundary condition [23]. The latter contains a positive parameter that can be used to enhance convergence. Optimized Schwarz methods find the best parameter through analytical techniques. For instance, a Fourier analysis of certain continuous elliptic partial differential equations, is performed in [7] (and references therein). In [6], there is numerical evidence that the weak Laplacian is spectrally close to the pseudo-Laplacian (11). Consequently, the construction of the various Schwarz preconditioners are based on a weak formulation of the Poisson problem.

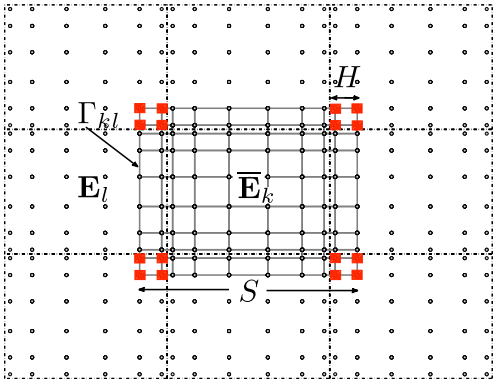

Fig. 1. One overlapping subdomain, $\bar{\mathbf{E}}_k$. Overlapping corner nodes are represented as red squares. $\mathbf{E}_l$, is a nonoverlapping neighboring element.

Suppose that the linear elliptic operator $\mathcal{L} := -\Delta$ with forcing f and boundary conditions $\mathcal{P} := \frac{\partial}{\partial \mathbf{n}}$ needs to be solved on $\mathbb{D}$. Then, an iterative algorithm that can be employed to solve the global problem $\mathcal{L}p = f$ is

$$\begin{aligned} \mathcal{L}p_k^{n+1} &= f \quad \text{in } \bar{\mathbf{E}}_k \\ \mathcal{P}(p_k^{n+1}) &= 0 \quad \text{on } \partial\mathbb{D}\cap\bar{\mathbf{E}}_k \text{ and } p_k^{n+1} = p_l^n \text{ on } \Gamma_{kl},\ \forall l \text{ s.t. } \partial\bar{\mathbf{E}}_k\cap\mathbf{E}_l \neq \emptyset \end{aligned} \tag{12}$$

where the sequence with respect to n will be convergent for any initial guess u^0. This is none other than the classical Schwarz algorithm at the continuous level corresponding to RAS at the matrix level. The optimized version of the above algorithm replaces the Dirichlet transmission conditions between subdomains by

$$\left[\frac{\partial p_k}{\partial \mathbf{n}} + T(p_k, r, q, \tau)\right]_{\Gamma_{kl}}^{n+1} = \left[\frac{\partial p_l}{\partial \mathbf{n}} + T(p_l, r, q, \tau)\right]_{\Gamma_{kl}}^{n} \tag{13}$$

where $T(p_k, r, q, \tau) \equiv rp_k - \frac{\partial}{\partial \tau}(q\frac{\partial p_k}{\partial \tau})$, defines a transmission condition of order 2 with two parameters, $r = r(x,y)$ and $q = q(x,y)$, with $r, q \geq 0$ on Γ_{kl} and $q = 0$ at $\partial\Gamma_{kl}$ as specified in [10]. The algorithm, like in the classical case, converges to the solution of $\mathcal{L}p = f$ with $\mathcal{P}(p) = 0$ on $\partial\mathbb{D}$ [23]. Its discrete algebraic version is

$$\tilde{A}_k \widehat{\boldsymbol{p}}_k^{n+1} = \begin{pmatrix} A_k^{ii} & A_k^{i\Gamma} \\ C_k^{\Gamma i} & C_k^{\Gamma\Gamma} \end{pmatrix} \begin{pmatrix} \widehat{\boldsymbol{p}}_k^{i} \\ \widehat{\boldsymbol{p}}_k^{\Gamma} \end{pmatrix}^{n+1} = \begin{pmatrix} f_k^i \\ f_k^\Gamma + C_k \widehat{\boldsymbol{p}}^n \end{pmatrix}$$

with $C_k^{\Gamma i}$, $C_k^{\Gamma\Gamma}$ and C_k corresponding to the discrete expressions of the optimized transmission conditions. At this point notice that A_k^{ii} is exactly the same block as in the original Schwarz algorithm. A simple manipulation leads to the following preconditioned system

$$\left\{ I - \sum_{k=1}^{K} R_{\mathbf{E}_k}^T \tilde{A}_k^{-1} \begin{pmatrix} 0 & 0 \\ 0 & C_k \end{pmatrix} R_{\bar{\mathbf{E}}_k}^T \right\} \widehat{\boldsymbol{p}} = \left\{ \sum_{k=1}^{K} R_{\mathbf{E}_k}^T \tilde{A}_k^{-1} R_{\bar{\mathbf{E}}_k} \right\} f \tag{14}$$

where $R_{\bar{\mathbf{E}}_k}$ and $R_{\mathbf{E}_k}^T$ are Boolean restriction and extension (by zero) matrices to the G quadrature points of element $\bar{\mathbf{E}}_k$ and $\mathbf{E}_k$, respectively. As seen in Fig. 1, two different overlapping domains can be considered. The first is cross-shaped (without corner nodes) and imposes optimized boundary conditions on $\partial\bar{\mathbf{E}}_k \backslash \{4 \text{ corner elements}\}$ and Dirichlet ones on the 4 corner elements represented by the square G quadrature points in Fig. 1. The second is the square (with corner elements) domain having optimized conditions on $\partial\bar{\mathbf{E}}_k$. The above results are completely algebraic and independent of the underlying space discretization method. The complete proof in the additive and multiplicative case with and without overlap can be found in [12]. Finally the one level optimized Schwarz preconditioned linear system (11) is

$$P_{ORAS}^{-1} E \widehat{\boldsymbol{p}}^{\pm,k-1} = P_{ORAS}^{-1} \mathbf{D}^j \widehat{\boldsymbol{g}}_j^{\pm,k-1} \tag{15}$$

where $P_{ORAS}^{-1} \equiv \{\sum_{i=1}^{K} R_{\mathbf{E}_i}^T \tilde{A}_i^{-1} R_{\bar{\mathbf{E}}_i}\}$ and k is the RK2 stage number.

4 Discretization of the Optimized Schwarz

In order to obtain the optimized preconditioner, it suffices to compute the matrices $\tilde{A}_k^{-1}$ in equation (14) from the model problem (12) at convergence ($p_k = p_k^n$) with the boundary condition (13). For simplicity, the *rhs* of the latter is set to g. Therefore the weak formulation of the problem is to find $u_k \in H^1(\bar{\mathbf{E}}_k)$ *such that*

$$\int_{\bar{\mathbf{E}}_k} \nabla\varphi \cdot \nabla p + \sum_{l \in nei_k} \int_{\Gamma_{kl}} \left(r\varphi p + q \frac{\partial \varphi}{\partial \tau_{kl}} \frac{\partial p}{\partial \tau_{kl}} \right) = \int_{\bar{\mathbf{E}}_k} \varphi f_k + \sum_{l \in nei_k} \int_{\Gamma_{kl}} \varphi g \tag{16}$$

for all $\varphi \in H^1(\bar{\mathbf{E}}_k)$. We introduce the tiling of the Gauss-Legendre quadrature points in element $\bar{\mathbf{E}}_k$ by $\Omega_h^k = \cup_{l=1}^{m_k} \mathbf{Q}_l$, and the finite dimensional space $V_k := \{v_h \in C^0(\bar{\mathbf{E}}_k) \mid v_h|_{\mathbf{Q}_l} \circ T_{\mathbf{Q}_l} \in (\mathbb{P}_1 \otimes \mathbb{P}_1)(\mathbf{Q}_l), \forall\, \mathbf{Q}_l \in \Omega_h^k\} \cap H^1(\bar{\mathbf{E}}_k)$. The basis used to represent polynomials in V_k are tensor products of the one dimensional linear hat functions $\varphi_i(\eta_j) = \delta_{ij}$ depicted in Fig. 2 at each Gauss-Legendre quadrature point $\{\eta_l\}_{l=-2}^{N}$. Using the one dimensional definition for the stiffness and lumped mass matrices,

$$K_{ij}^k := \int_{\eta_{-2}}^{\eta_N} \frac{d\varphi_i}{d\eta} \frac{d\varphi_j}{d\eta} d\eta \quad \text{and} \quad M_{ij}^k := \int_{\eta_{-2}}^{\eta_N} \varphi_i(\eta)\varphi_j(\eta) d\eta,$$

respectively, leads to the following tensor product representation of (16):

$$\begin{aligned} \tilde{A}_k := (K^k + T^k_{r_b,r_t}) \otimes (M^k + T^k_{q_l,q_r}) + (M^k + T^k_{q_b,q_t}) \otimes (K^k + T^k_{r_l,r_r}) \\ - T^k_{r_b,r_t} \otimes T^k_{q_l,q_r} - T^k_{q_b,q_t} \otimes T^k_{r_l,r_r}. \end{aligned} \tag{17}$$

In the last expression, $T^k_{a,b}$ is a matrix with only two non-zero entries at $(1,1)$ and (N,N), which are set to a and b respectively. The notation $q_{r,l,b,t}$ stands for the q optimized parameter at either the right, left, bottom or top boundaries (*idem* for parameter r).

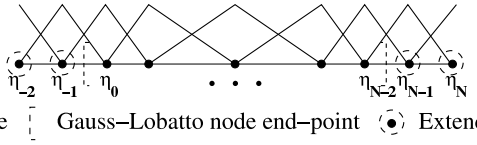

Fig. 2. Schematic of the assembly procedure.

	r	q
OO0, overlap H	$2^{-1/3}(k_{\min}^2)^{1/3}H^{-1/3}$	0
OO2, overlap H	$2^{-3/5}(k_{\min}^2)^{2/5}H^{-1/5}$	$2^{-1/5}(k_{\min}^2)^{-1/5}H^{3/5}$

Table 1. Parameters r and q used in the transmission blocks. $k_{\min} = \pi/S$ with S the characteristic size of the element normal to the face where the parameters are required.

When rectangular elements are considered the FDM (e.g., [3]) can be used to invert the optimized blocks. The number of operations required to invert $N^d \times N^d$ matrix using such a technique is $O(N^{d+1})$ and the application of the inverse is performed using efficient tensor products in $O(N^{d+1})$ operations. We propose the form derived in (17) with the r and q parameters constant on their respective faces but eliminating the last two terms of the form $T^k_{:,:} \otimes T^k_{:,:}$. This is done in order for the fast diagonalization technique to be applicable. Indeed, the modified mass matrix $M^k + T^k_{:,:}$ is still symmetric and positive definite while the matrix $K^k + T^k_{:,:}$ is still symmetric. This enables the use of the modified mass matrix in an inner product and the simultaneous diagonalization of both tensors. When $q = 0$, the proposed formula is exact.

5 Numerical Experiments

The RAS preconditioner described above was implemented in the MHD code. This version allows for variable overlap of the extended grid. The ORAS counterpart has also been implemented as described, and for comparison, we use a high-order block Jacobi (BJ). We consider first tests of a single pseudo-Poisson solve on a $[0,1]^2$ bi-periodic domain with exact solution $p = \cos(2\pi x)\cos(2\pi y)$. In the first experiment, we use a grid of $E = 8 \times 8$ elements, and iterate using BiCGStab until the residual is 10^{-8} times that of the initial residual. The extended grid overlap is 2, and the initial starting guess for the Krylov method is composed of random noise.

The first test uses non-FDM preconditioners to investigate the effect of including corner transfers on the optimization. The results are presented in Fig. 3, in which we consider only the OO0 optimization. Note that even though the RAS is much less sensitive to the subdomains without corners, especially at higher N_v, the OO0 with subdomains including corners requires fewer iterations. Clearly, including the corners is crucial to the proper functioning of the optimized methods.

In the second experiment, all the parameters are maintained except we use a grid of $E = 16 \times 16$ elements together with the FDM version of the preconditioners to investigate performance. These results are presented on the right-most figure of Fig. 3.

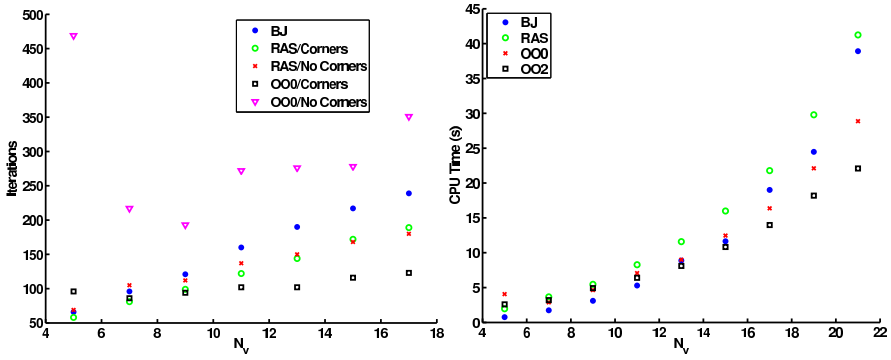

Fig. 3. *Left:* Plot of iteration count vs GLL-expansion node number for different preconditioners using subdomains with and without corners on an 8×8 element grid. *Right:* Comparison of of CPU time vs. GLL-expansion node number of FDM-based preconditioners with subdomain including corners on a 16×16 element grid.

Acknowledgement. NCAR (National Center for Atmosphereic Research) is supported by the National Science Foundation. S.D. Kim was supported by award KRF-2008-313-C00094.

References

[1] Canuto, C., Hussaini, M.Y., Quarteroni, A., Zang, T.A.: *Spectral methods in fluid dynamics*. Springer, 1988.

[2] Chniti, C., Nataf, F., Nier, F.: Improved interface condition for 2D domain decomposition with corner : a theoretical determination. Technical Report hal-00018965, Hyper articles en ligne, 2006.

[3] Couzy, W.: *Spectral element discretization of the unsteady Navier-Stokes equations and its iterative solution on parallel computers*. PhD thesis, École Polytechnique Fédérale de Lausanne, 1995.

[4] Deville, M.O., Fischer, P.F., Mund, E.H.: *High-Order Methods for Incompressible Fluid Flow*. Cambridge University Press, 2002.

[5] Elsässer, W.M.: The hydromagnetic equations. *Phys. Rev.*, 79:183, 1950.

[6] Fischer, P.F.: An overlapping Schwarz method for spectral element solution of the incompressible Navier-Stokes equations. *J. Comput. Phys.*, 133:84–101, 1997.

[7] Gander, M.J.: Optimized Schwarz methods. *SIAM J. Numer. Anal.*, 44(2):699–731, 2006.

[8] Lions, P.-L.: On the Schwarz alternating method. I. In R. Glowinski, G.H. Golub, G.A. Meurant, and J. Périaux, eds., *First International Symposium on Domain Decomposition Methods for Partial Differential Equations*, pages 1–42, Philadelphia, PA, 1988. SIAM.

[9] Maday, Y., Patera, A.T., Rønquist, E.M.: The $\mathbb{P}_N$-$\mathbb{P}_{N-2}$ method for the approximation of the Stokes problem. Technical report, Pulications du Laboratoire d'Analyse Numérique, Université Pierre et Marie Curie, 1992.

[10] Nataf, F.: Interface connections in domain decomposition methods. In A. Bourlioux and M.J. Gander, eds., *Modern Methods in Scientific Computing and Applications*, vol. 75 of *NATO Science Series II*, pages 323–364. Kluwer Academic, 2001.

[11] Rosenberg, D., Pouquet, A., Mininni, P.D. Adaptive mesh refinement with spectral accuracy for magnetohydrodynamics in two space dimensions. *New J. Phys.*, 9(304), 2007.

[12] St-Cyr, A., Gander, M.J., Thomas, S.J. Optimized multiplicative, additive, and restricted additive Schwarz preconditioning. *SIAM J. Sci. Comput.*, 29(6):2402–2425, 2007.